Check for
updates

A Consideration of Radioxenon Detections Around the Korean Peninsula

M. A. Goodwin,[1] R. Britton,[1] and A. V. Davies[1]

Abstract—The detection of radioxenon isotopes from an underground nuclear test using the International Monitoring System of the Comprehensive Nuclear Test-Ban Treaty is complicated by a radioxenon background, largely originating from the civil radioxenon emissions of medical isotope production facilities and nuclear power plant reactors. Much of the background is measured as single isotopes near the detection threshold, limiting the use of isotopic ratios which could differentiate between the possible sources. Here we introduce the UK Radionuclide National Data Centre methodology to approach the problem of radioxenon detections and source identification. Using automated analysis of radiometric data and atmospheric transport simulations, the detectability of radioxenon isotopes ^{133}Xe, ^{131m}Xe, ^{133m}Xe and ^{135}Xe from North Korea is estimated for the Takasaki radionuclide station JPX38, and the possibility of detecting ^{133}Xe from selected locations across the Korean Peninsula and extended region is investigated.

Keywords: CTBT, radioxenon, radionuclide, IMS, DPRK, nuclear, test, verification, regime.

1. Introduction

The Comprehensive Nuclear Test-Ban Treaty (CTBT) International Monitoring System (IMS) provides a network of 336 facilities spread worldwide, including 120 radionuclide (RN) detection stations, strategically positioned at 80 sites with the aim of detecting radionuclide emissions from nuclear explosions (see Fig. 1) (UNGA 1996).

The IMS is designed to detect nuclear explosions using a variety of different measurement techniques (Matthews and Schulze 2001), but this work focusses on the methods used for detecting radioactive isotopes produced during (and after) the explosion. When conducting a nuclear test, fission processes

produce a large number of isotopes including noble gases. Of those isotopes produced, some are able to be detected thousands of kilometres from the source (Bowyer et al. 2013). The most likely materials to escape an underground nuclear test are noble gases, due to the elements being chemically inert, volatile and (in some cases) the radionuclides are sufficiently long-lived. For these reasons, the radioxenon isotopes ^{133}Xe, ^{133m}Xe, ^{131m}Xe and ^{135}Xe are all CTBT relevant radionuclides (De Geer 1999; Bowyer et al. 2002). Detections of multiple isotopes can be used to infer the type of fission process that has taken place, and whether it is linked to a reactor or weapon (Kalinowski et al. 2010).

To date, the Democratic Peoples Republic of Korea (DPRK) have announced six nuclear weapon tests and the IMS has been partially successful in detecting associated signals in the form of radioxenon isotopes. Detections that have been associated with a release from an underground nuclear test (UGT) had activity concentrations close to the detection limit of the measurement system, but the identification of more than one isotope made isotopic activity ratio analysis possible (Ringbom et al. 2014).

The International Noble Gas Experiment (INGE) have demonstrated the presence of a significant (and dynamic) global radioxenon background, which contributes to radiometric measurements of xenon isotopes in air samples, especially in the Northern hemisphere (Bowyer et al. 2013; Saey 2009; Hoffman and Berg 2018; Kalinowski and Tuma 2009; Achim et al. 2016). A number of civil facilities producing the radioxenon background are present in the region around North Korea and hence have an effect on the ability of the IMS to detect radioxenon from a DPRK nuclear test. Given the possibility of regional IMS radioxenon detections originating from a DPRK nuclear test, it is important to understand any other
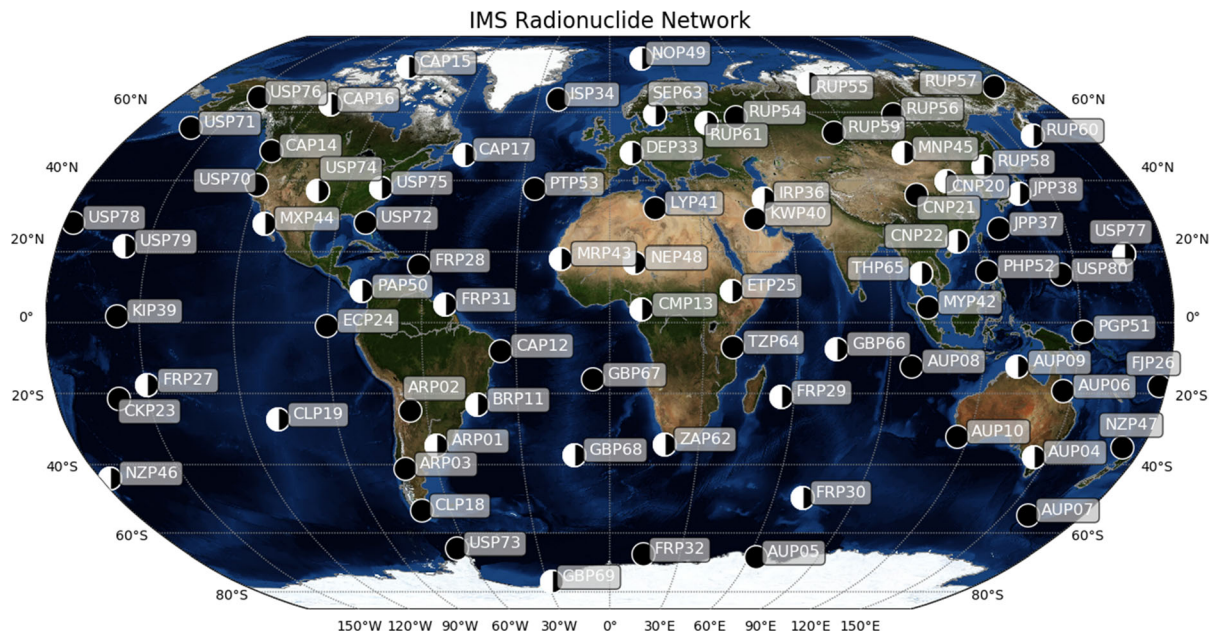
Figure 1
The International Monitoring System Radionuclide Network. Half-filled markers represent the stations with a noble gas capability (or planned capability). When complete, the RN network will consist of 80 sites, all with particulate detection technology. At present, there are only plans for half of the network to utilise noble gas analysis technology

contributions to radioxenon detections that may affect the conclusions drawn by States Parties to the CTBTO.

In this work we have used the operational tools in place at the UK National Data Centre (NDC) to consider other contributors of radioxenon around the Korean Peninsula, focussing on the DPRK Yongbyon Nuclear Reactor and two Chinese Medical Isotope Production Facilities (MIPFs).

Werth et al. have considered the effect of known sources of radioxenon on IMS stations in the region by quantifying the signal from the DPRK test site compared to signals from various known emitters. They compared the overlap of simulated plumes from each source (emitted continuously) to determine whether they remain distinct from one another. The authors concluded that radionuclide signals from the test site usually remain distinct from other simulated signals and that a DPRK emission need not be significantly higher than nearby sources in order to be detected. This work did not include simulated emissions from the North Korean Yongbyon reactor,

located relatively close to the Punggye-ri test site (Werth and Buckley 2017).

Through the analysis of radioxenon collected and measured at JPX38 (Takasaki, Japan) as well as combining Atmospheric Transport Modelling (ATM) simulations, we compare the possibility of IMS radioxenon detections originating from the DPRK test site with other locations in the area, including the Yongbyon nuclear facility. Of the 25 certified noble gas stations currently operating on the IMS, JPX38 is considered the most appropriate station to study the sensitivity to radioxenon emissions from the DPRK. This is based on a high reliability and uptime and close proximity to the DPRK test site compared with other stations in the area (see Table 1). A preliminary assessment of the atmospheric transport and operating stations in this region indicated JPX38 to be the (CTBTO noble gas certified) station most likely to receive a contribution of radioxenon above a nominal dilution factor of 1E−15.

Through careful consideration of a number of scenarios and ATM simulation, we evaluate the probability of detecting and quantifying the CTBT

Table 1

Distances of the closest 10 noble gas IMS stations from the DPRK test site, showing the detector technology type and current capability status

Station	Distance (km)	System type	Status
X58	396.1	ARIX	Installed
X38	1026	SAUNA	Certified
X20	1082	SPALAX	Installed
X45	1939	SPALAX	Certified
X22	2503	SAUNA	Installed
X60	2570	ARIX	Installed
X55	3930	–	Preparation
X65	4137	–	Preparation
X77	4303	SAUNA	Certified
X09	5978	SAUNA	Certified

Current status defined in the most recent PTS report (PTS Report 2020)

(radioxenon) relevant radionuclides at this location from a number of possible emitters in the region, using UK NDC operational tools. The RN analysis and ATM simulation pipelines are introduced in Sect. 2, a nuclear test scenario is modelled in Sect. 3, the ATM simulations of emissions from the test site as well as other locations are discussed in Sect. 4 and the analysis of real RN detections at JPX38 is given in Sect. 5.

2. Analysis at the UK National Data Centre

Since 2004, AWE Aldermaston has operated the CTBT-certified radionuclide laboratory GBL15, as part of the IMS RN network supporting the CTBT Verification Regime (Comley and Price 2003). In 2017 this capability was enhanced, with the certification of the noble gas capability at GBL15, specialising in the measurement of radioxenon isotopes (INF96 2012). The UK National Data Centre (NDC) is also hosted by AWE, with the RN component co-located with GBL15. The NDC is a technical organisation providing appropriate information to the UK Government.

At the NDC and GBL15, UK RN experts have developed a number of software tools, including fully automated pipelines for the analysis of IMS radionuclide data and ATM simulations (see Fig. 2). There are a number of complementary technologies within the IMS that are used to detect nuclear explosions, with seismic, infrasound and hydroacoustic technologies also used. For all but the largest of nuclear tests, radionuclide detection remains the gold standard for confirming a nuclear origin. In this study, analysis is limited to radionuclide detection and associated ATM; the fusion of waveform data is beyond the realms of this paper.

2.1. Radionuclide Pipeline

The RN Pipeline is a custom pipeline dedicated to the analysis of all radiometric data gathered on the IMS. The pipeline is automatically activated daily and analyses the data through a number of custom scripts and software packages. Particulate analysis is completed using the GBL15-developed Genie Gamma Analysis for Particulate data (GGAP). This code makes use of the Universal Software Development Kit (U-SDK) developed by Mirion Technologies in order to analyse the high resolution γ spectra of air filters using GBL15 analysis procedures and nuclear libraries. A number of meta-analyses are applied to the results in order to implement extra logic such as interference corrections for ^{99m}Tc/^{75}Ge & ^{208}Tl/^{54}Mn etc.

Noble gas analysis is divided into two, since there are currently two methods for measuring the relevant isotopes on the IMS (Auer et al. 2004). The first type is $\beta - \gamma$ coincidence spectrometry, such as that used in the SAUNA (Ringbom et al. 2003) and SPALAX-NG (Cagniant et al. 2018). The second is high resolution singles γ measurements, using a High Purity Germanium (HPGe) detector, such as the current SPALAX generation (Fontaine et al. 2004).

The UK NDC developed a code for the Beta-Gamma Analysis of Radioxenon data (BeGAX), which utilises a modified Net Count Calculation (NCC) analysis method (sometimes known as the ROI method) (Deshmukh et al. 2017). The method was developed based on the *Stockholm equations* and modified in order to reduce false positives and enhance performance (Axelsson and Ringbom 2003, 2014).
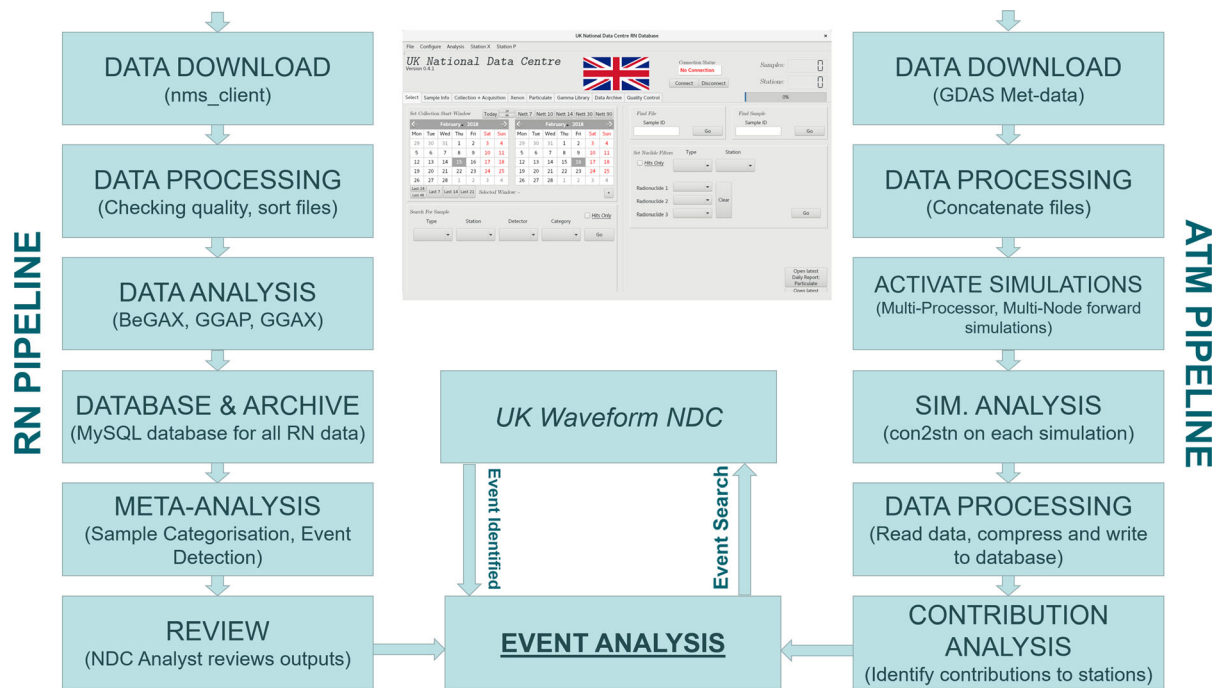
Figure 2
Flow diagrams for the Radionuclide and ATM pipeline running at the UK NDC. The RN Pipeline (left) makes use of a download client (nms_client) provided by the International Data Centre (IDC), and then custom codes for analysis. Centre is the graphical user interface (GUI) used for assessing RN events

Analysis of singles γ spectra from radioxenon measurements is completed using the UK NDC developed Genie Gamma Analysis for Xenon (GGAX). Similar to GGAP, the code uses the U-SDK and then applies extra meta-analysis in order to identify the four radioxenon isotopes of interest from the γ and X-ray emissions.

All data from the RN Pipeline is captured and archived in a SQL database. All results are post-processed in order to categorise the results based on magnitudes, isotopic hit-patterns and station history, which is then used to inform and direct the analysis at the NDC. Results from the automated activity concentration analysis of radioxenon data from JPX38 over time is shown in Fig. 3.

2.2. Atmospheric Transport Modelling Pipeline

ATM can be utilised to calculate contributions from different regions to the sampled air at the
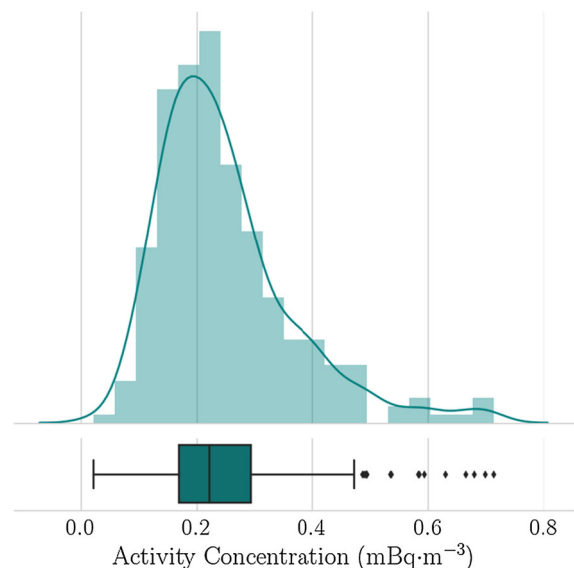

Figure 3
Station history frequency & box plot for ^{133}Xe detections at JPX38 for December 2018–December 2019. The plot highlights the majority of detections are below 0.5 mBq.m^{-3}

Table 2

Simulation properties for the ATM pipeline forward modelling

Description	Value	Units
N particles/release	100,000	
Max particles	100,000	
Rate	13.9	part s^{-1}
Release Duration	2	h
Stack Height	40	m
Wet deposition	OFF	
Dry deposition	OFF	
Emission release times	0300, 0900, 1500, 2100	h
Max Sim. height	10,000	m
Sampling layer	0–200	m
Sampling spatial res.	0.5 & 1.0	°
Sampling temporal res.	1.0	h
Met. spatial res.	0.5 & 1.0	°
Met. temporal res.	3.0	h

radionuclide stations. The Hybrid Single-Particle Lagrangian Integrated Trajectory (HYSPLIT) model, developed by NOAA's Air Resources Laboratory (ARL), is one such tool to conduct ATM (Stein et al. 2015).

At the UK NDC, an IMS station contribution is calculated to evaluate the sensitivity of a radionuclide station to (simulated) civil radionuclide emissions, including known facilities such as Medical Isotope Production Facilities (MIPFs) and Nuclear Power Plants (NPPs). The model parameters of the pipeline simulated emissions are given in Table 2. The station contribution is a concentration value, referenced to a specific emission. Effectively, it describes the fraction of the RN emission that is present at the station location, averaged over a height of 200 m. The HYSPLIT *con2stn* program is used to extract the concentration values from the binary simulation data file.

From continuous modelling of noble gas radionuclide emissions from known sources and locations of interest (Table 3), a database of station contributions has been compiled. The database contains the contribution data from four emissions per emitter, per day, at every IMS station using both 1.0° and 0.5° resolution meteorological data, for every day from 2010 to the current week.

Figure 4 shows a visualisation of the simulated emissions from the DPRK test site and Yongbyon

nuclear reactor. The plumes are visibly combined at the point they reach JPX38 and this is often reflected in the average station contribution factors, which affect the station at roughly the same time. For any given station, the contribution from any given simulation is often viewed in 2D plots, such as those shown and discussed in Fig. 5

2.3. Data Fusion and Event Analysis

The emitters listed in Table 3 are compiled from a variety of open sources. Only emitters with status '1' are routinely modelled, any with status '0' are only modelled for special studies such as this one. This list of locations is by no means exhaustive, but includes a selection of the world's MIPFs and emitters that may affect noble gas IMS stations. Emitters 19–25 were added to support this work in understanding the radioxenon contributors to JPX38. RAdioxenon Station Contribution Analysis (RASCA) is a tool to evaluate the data stored in the ATM database. The code is focussed on reading and summing relevant contributions to a station, from a number of emitting sources, quantifying the total contribution and flagging those above a cut-off value. The database contains a filtered selection of emissions that contribute to IMS stations with a critical dilution factor above the threshold value (1E−15). This has made it possible to correlate simulated emissions of noble gas radionuclides with measured data collected at IMS stations.

The RN and ATM pipelines are fused by overlaying RN events with simulated contributions from modelled emitters. This involves cross-comparing the detections at JPX38 with the filtered simulated contributions and flagging emissions that match the collection time of the identified radionuclides. Each detection event is often contributed to by more than one pipeline emission, for example a detection at an IMS station has two or more simulated emissions from different emitters flagged as possible contributers for the detection event collection period. It is important to remember that the pipeline emissions take place at fixed times, which are not necessarily representative of any real emissions from these locations, but are able to show that the station is 'sensitive' to the emitters during a collection period.

Table 3

A selection of radioxenon emitters (and sites of interest) relevant to the IMS noble gas RN network, modelled in the ATM pipeline

Emitter ID	Emitter name	Emitter desc	Latitude	Longitude	Status
1	SA1	Pelindaba SA (NTP)	− 25.480	27.560	1
2	BE1	IRE Belgium	50.270	4.320	1
3	PK1	PINSTEC Pakistan	33.390	73.150	1
4	AU1	ANSTO Australia	− 34.050	150.980	1
5	CA1	Nordion Canada	45.340	− 75.910	1
6	AR1	CNEA Argentina	− 34.820	− 58.580	1
7	CN1	HFETR China	29.750	103.670	1
8	RU1	Karpov Institute Russia	55.750	37.650	1
9	DPRK	DPRK Test Site	41.290	129.110	1
10	CARR	CARR China (RIAR)	39.440	116.030	1
11	IBAM	Mallinckrodt US	38.660	− 90.190	1
12	NK1	DPRK reactor Yongbyon	39.790	125.750	1
13	SE1	Forsmark Sweden	60.403	18.167	1
14	JP1	Ikata Japan	33.490	132.310	1
15	JP2	Sendai Japan	31.820	130.190	1
16	JP3	Takahama Japan	35.520	135.500	1
17	JP4	Tomari Japan	43.040	140.510	1
18	JP5	Oma Japan	41.510	140.910	1
19	CH1	Hongyanhe China	39.790	121.480	0
20	CH2	Tianwan China	34.690	119.460	0
21	CH3	Qinshan China	30.430	120.950	0
22	SK1	Hanbit South Korea	35.410	126.420	0
23	SK2	Wolseong South Korea	35.710	129.480	0
24	SK3	Hanul South Korea	37.090	129.380	0
25	SK4	Kori South Korea	35.320	129.290	0

The 'status' does not reflect the true status of the emitter, but represents the current simulation status. Japanese NPPs are selected using referenced report (IAEA Report 2019)

Figure 5 shows the pipeline simulated contributions to JPX38 from the DPRK test site during a time when a number of samples containing measurable quantities of ^{133}Xe were collected. Pipeline simulations for the Yongbyon nuclear reactor also show station contributions during the same period, with emissions starting at 31/12/2017 12:00 and 31/12/2017 21:00 contributing to the station most. The events flagged in this part of the automated analysis have been used to evaluate the source of detections at JPX38 (see Sect. 5).

Data fusion involves the combination of the average contribution dilution factor from the forward ATM simulation with the measured radionuclide activity concentrations in order to calculate a radionuclide source-term (the activity of radionuclides emitted from the source). Given A_c ranges from ~ 0.1 to ~ 1.0 (> 95 %), the source-term is very much dependent on the dilution factor F which varies by several orders of magnitude. The source-

term (S) is estimated through Eq. (1) where F is calculated from the average source emission contribution over the collection period.

$$S = \frac{A_c}{F} \qquad (1)$$

Using the thousands of emissions and station contribution calculations in the ATM database, a 'hit map' is being collated to show which stations are sensitive to which facilities modelled in the pipeline. This is used to guide the UK NDC scientists when investigating the source of a radionuclide detection event.

3. Simulating Nuclear Test Scenarios

Many emitters of radioxenon publish yearly emissions data which can be useful when attempting to predict a contribution to a station. When a nuclear test takes place, there are many factors that affect the
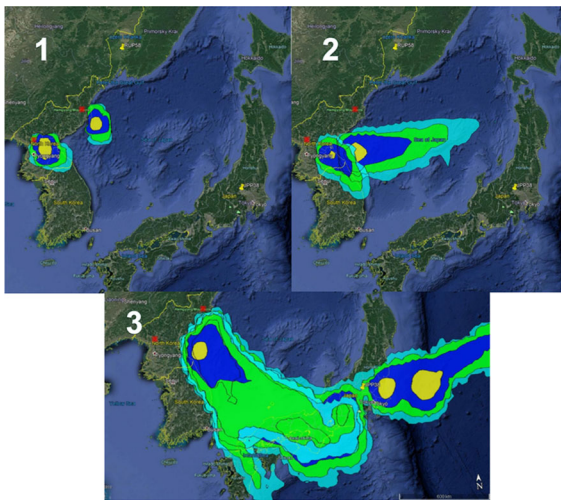
Figure 4
Pipeline simulations for DPRK locations a) Punggye-ri Test Site and b) Yongbyon Nuclear Reactor; proceeding in chronological order 1–3. Simulations shown using Google Earth
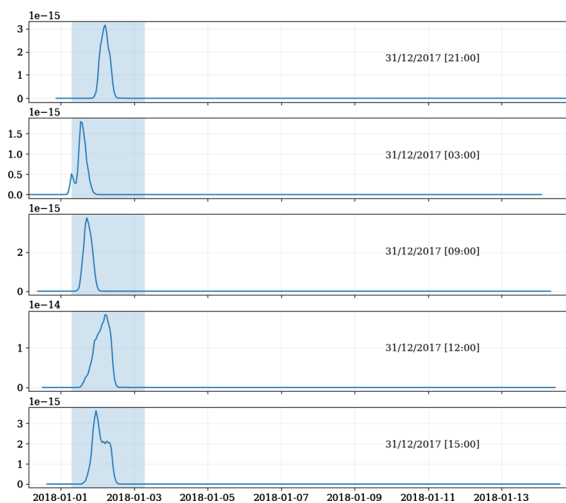

Figure 5
Example for simulated contributions to JPX38 from the DPRK test site, where the emission start time is shown on each plot. Multiple simulations were highlighted by the pipeline with contributions to JPX38 during an identified RN 'event'. The shaded blue period represents the back-to-back collection periods where ^{133}Xe was detected at JPX38

magnitude and composition of a radionuclide emission to the atmosphere. To understand the sensitivity of an IMS station to a site that may be conducting a nuclear explosion, it is necessary to consider the detectability of radionuclides that could be released

during the event. The materials present in the device affect the quantities and ratios of isotopes produced during nuclear fission, and the containment of these radionuclides (and subsequent fractionation) can greatly modify this inventory when collected on the IMS.

For the purpose of this study, the scenario considered was based on ^{239}Pu fission, so appropriate yields from England and Rider have been applied and the decay and ingrowth of the relevant radionuclides modelled to find an *effective yield* (England and Rider 1993). The cumulative fission yield may not be an appropriate measure of the radionuclides present due to unknowns in the containment and fractionation of the fission inventory. All calculations are completed using the GBL15 developed software package NuDIC (Nuclear Decay Iterative Calculator).

Taking a variety of release times and allowing a fixed transport time for the atmosphere to transport the radionuclides to Takasaki (around 1 day post-fractionation), then we may express the detectability of ^{133}Xe at JPX38 as a function of both weapon yield (kt) and release fraction. Based on these assumptions, a vented fraction of around 5E−5 is required for a 100 kT explosion, in order to detect ^{133}Xe at JPX38 (see Fig. 6). These calculations ignore the effects of slow seepage from the ground and a mean dilution factor 1E−15 is used as a mean dilution factor to estimate the amount of released material that is collected at JPX38.

The concentration of radioxenon measured at a station can be calculated using Eq. (2), where *fiss* is the number of fissions from the weapon, λ is the decay constant (s^{-1}) Y is the cumulative nuclide fission yield at the release time, R is the release fraction, F is the dilution factor, t is the decay time from release to collection.

$$C = fiss \cdot \lambda \cdot Y \cdot R \cdot F \cdot e^{-\lambda \cdot t} \qquad (2)$$
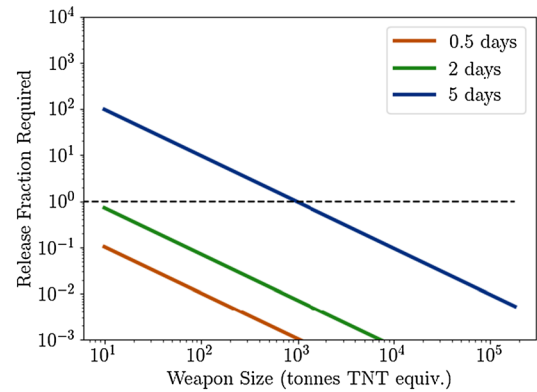
Given the number of fissions associated with 1 tonne equivalent nuclear explosion, we derive the tonne-release fraction product (TR)

$$TR = \frac{C}{\lambda \cdot Y \cdot F \cdot e^{-\lambda \cdot t} \cdot 1.46 \times 10^{20}} \qquad (3)$$
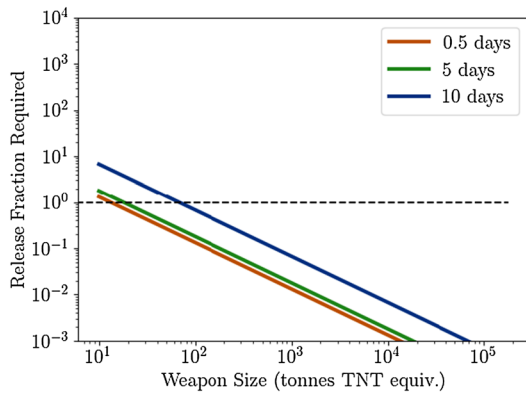
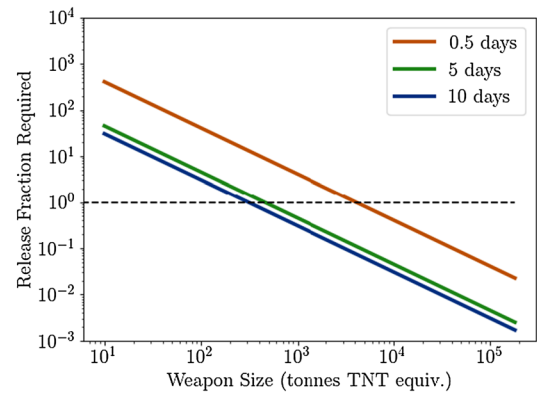By representing *TR* as a function of the weapon TNT equivalent (tonnes) and the release fraction (0...1),
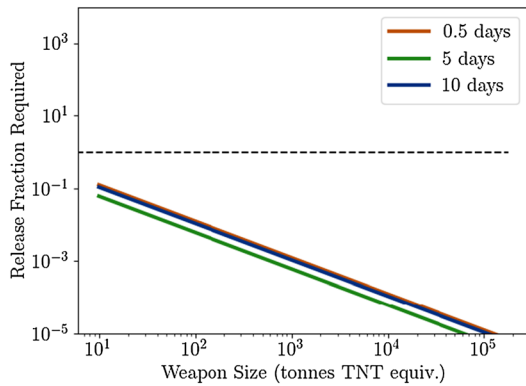
(a) Weapon size and Release fraction requirements for detections of ^{133}Xe at JPX38

(b) Weapon size and Release fraction requirements for detections of ^{135}Xe at JPX38

(c) Weapon size and Release fraction requirements for detections of ^{133m}Xe at JPX38

(d) Weapon size and Release fraction requirements for detections of ^{131m}Xe at JPX38

Figure 6

Weapon size and release fraction requirements for detections of all four radioxenon isotopes of interest at JPX38, following a release from the North Korean test site and varied release time after the explosion. The dashed line represents 100% release, whilst the coloured lines represent the lower bound of detection for various release times. 'Detection' would therefore be likely in the envelope between the coloured lines and the dashed line, but can only occur below the dashed line. **a** Weapon size and Release fraction requirements for detections of ^{133}Xe at JPX38. **b** Weapon size and release fraction requirements for detections of ^{135}Xe at JPX38. **c** Weapon size and release fraction requirements for detections of ^{133m}Xe at JPX38. **d** Weapon size and release fraction requirements for detections of ^{131m}Xe at JPX38

where the concentration is fixed to the minimum detectable concentration (MDC) of a given radionuclide (Table 4), we can illustrate the scenarios which will result in quantifiable detections of each radioxenon isotope. 1.46E+20 is the number of fissions per tonne equivalent (Miskel 1964).

Figure 6 shows the variation in the release fraction required with increasing yield of explosion for different decay times. The dashed line shows a release fraction of 1 (100%), so any combination of T and R with $TR = const$ above this line can not be

Table 4

Mean MDCs of IMS radioxenon isotopes of interest at JPX38, based on pipeline results in the UK NDC RN database

Radionuclide	MDC (mBq m^{-3})
^{133}Xe	0.28
^{131m}Xe	0.14
^{133m}Xe	0.14
^{135}Xe	0.87

detected at JPX38 in this simulation, as more than 100% of the inventory would need to be released. Given the time taken for ^{131m}Xe (an important radionuclide used in the discrimination of civil and non-civil detections (see Kalinowski et al. 2010)) to grow in from ^{131}I, a longer time period before fractionation is preferred, but this hinders the detection of shorter lived fission products such as ^{135}Xe.

The values in Table 4 are used to determine whether a quantifiable activity is present at the station under the modelled scenarios. The MDC is calculated using the Currie method (Currie 1968) and 12 h background $\beta - \gamma$ coincidence acquisitions, completed twice every 24 h.

For the weapon sizes considered, this simulation demonstrates the high likelihood of detection of ^{133}Xe from the test site (primarily due to high fission yield and long-enough half-life) and that the other 3 isotopes have varying detectability, depending on emission magnitude and decay/ingrowth time. In reality, the collection and identification of all 4 isotopes in a single sample of radioxenon originating from the test site, can only occur in a small window of time and circumstance. In order to compare the likelihood of emissions from the test site being detected with that of civil emissions, a value of 1E+14 Bq is used, which roughly represents 0.1 % release of ^{133}Xe from a 1 kT explosion at 4 days post-detonation. Any debris from a DPRK nuclear test is often well contained, so this example would represent a significant release but is used for the purpose of comparison. The following section compares the detectability of an emission of this magnitude from the test site, with that of the estimated average emissions from other sites.

4. Atmospheric Background: Characterising a Radioxenon Source

With regards to the JPX38 station, there are several known emitters that may be contributing to the radioxenon background at this location, and potentially triggering radioxenon detections. Some of these emitters are displayed on the map shown in Fig. 7. China Advanced Research Reactor (CARR) and High Flux Engineering Test Reactor (HFETR) produce
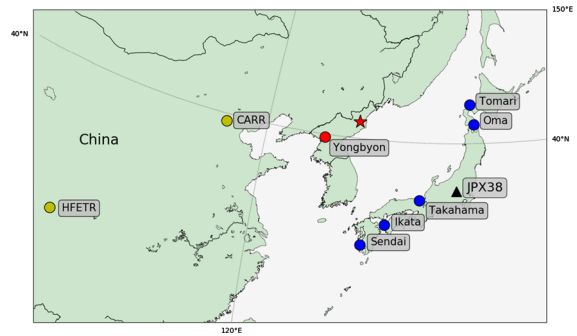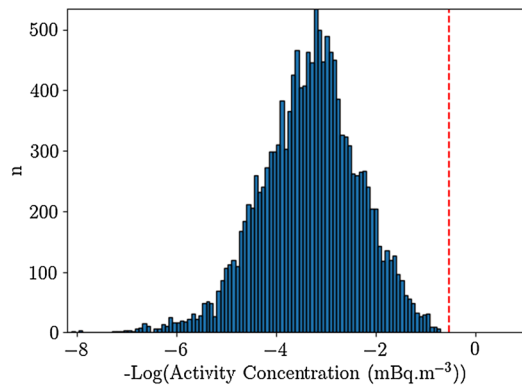

Figure 7
Map of Eastern Asia, showing the location of Chinese MIPFs (yellow), DPRK facilities (red), Japanese NPPs (blue) and the JPX38 IMS station (black triangle). The DPRK Punggye-ri test site is marked with a red star

^{99}Mo and other radioisotopes and are a large source of atmospheric ^{133}Xe. Here we consider the simulated emissions from the Chinese MIPFs and DPRK sites, as a possible source of interference with simulated emissions from the DPRK test site. These locations have been selected based on the magnitude of ^{133}Xe emission from MIPFs, and the locality of Yongbyon to the Punggye-ri test site.
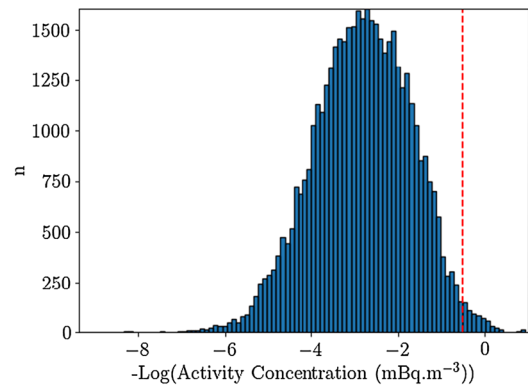
Given the literature average daily emissions from nuclear reactors it is possible to represent the likelihood of radioxenon originating from a given source through ATM simulation, based on the location and estimated magnitude of source. Histograms shown in Figs. 8a and 8b give the distribution of contribution factors from CARR and HFETR MIPFs. By utilising the ATM database and the modelled contributions to each station, we assess the possibility of each facility contributing to the JPX38 ^{133}Xe background. All simulations generated and discussed in this section were for the year of 2018 and are based on ^{133}Xe.

Figure 8d shows the distribution of contributions to JPX38 from a modelled emission of radioxenon from the DPRK test site. It shows that emissions of 1E+14 Bq will contribute to a detection at JPX38 in more than 50% of instances.

Based on this study, it is apparent that no emissions of magnitude 1E+10 Bq from the Yongbyon Reactor can explain detections at JPX38 (see Fig. 8c), without attempting to combine the signals of multiple emitters. Of course, the magnitude is a fixed emission value calculated from literature averages (see Kalinowski and Tuma 2009) and may not be
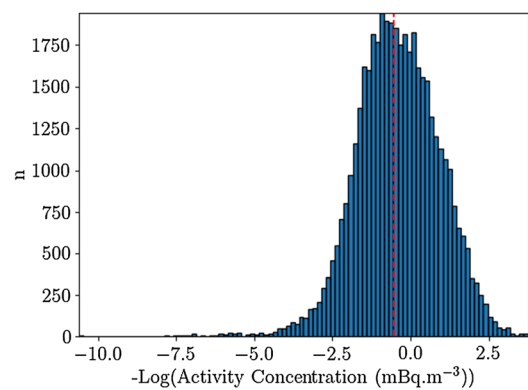
(a) HFETR - JPX38 Simulated activity concentration distribution showing the range of modelled activities, based on a release of 1E+12 Bq ^{133}Xe

(b) CARR - JPX38 Simulated activity concentration distribution showing the range of modelled activities, based on a release of 1E+12 Bq ^{133}Xe
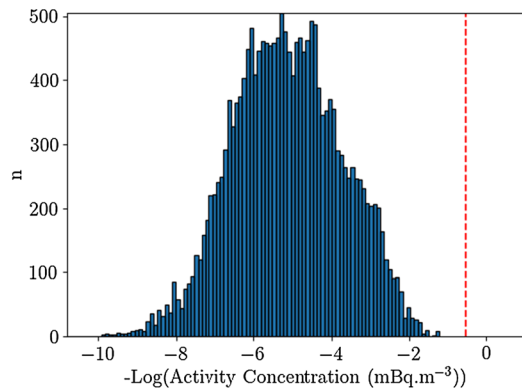
(c) Yongbyon - JPX38 Simulated activity concentration distribution showing the range of modelled activities, based on a release of 1E+10 Bq ^{133}Xe

(d) North Korean Test site - JPX38 Simulated activity concentration distribution showing the range of modelled activities, based on a release of 1E+14 Bq ^{133}Xe

Figure 8

Source: JPX38 contribution distributions, showing the projected measured activity at JPX38 for each collection period and for each simulation based on a release of ^{133}Xe. The detection limit is plotted as a dashed red line (0.28 mBq m^{-3} for ^{133}Xe). **a** HFETR: JPX38 Simulated activity concentration distribution showing the range of modelled activities, based on a release of 1E+12 Bq ^{133}Xe. **b** CARR: JPX38 simulated activity concentration distribution showing the range of modelled activities, based on a release of 1E+12 Bq ^{133}Xe. **c** Yongbyon: JPX38 Simulated activity concentration distribution showing the range of modelled activities, based on a release of 1E+10 Bq ^{133}Xe. **d** North Korean Test site: JPX38 simulated activity concentration distribution showing the range of modelled activities, based on a release of 1E+14 Bq ^{133}Xe

representative. Based on UK NDC RN and ATM pipelines, multiple RN events at JPX38 have been linked to the Yongbyon facility. Given the lack of another known facility that would explain these detections, it is likely that Yongbyon is emitting and contributing to JPX38. Given magnitudes of greater than 1E+10 Bq are required, the following section discusses the estimation of a Yongbyon source-term, using various real RN events at JPX38.

5. Linking IMS Noble Gas Measurements to Potential Sources

During January and February 2018, the UK NDC automated RN Pipeline flagged a number of ^{133}Xe detections to radionuclide experts. The automated results are given in Table 5. These particular results were highlighted by the review & categorisation codes due to the back-to-back detection of pure ^{133}Xe above MDC during a period where the ATM

Table 5

January–February 2018 Detections of Interest at JPX38, along with source-term calculations from most appropriate ATM Pipeline simulation(s)

Collection start	Activity concentration (mBq m^{-3})	Mean contr. factor (m^{-3})	Source-term (Bq)
2018/01/01 07:00	0.226	–	–
2018/01/01 19:00	0.555	7.11E−16	7.81E+11
2018/01/02 07:00	0.675	1.20E−15	5.63E+11
2018/01/02 19:00	0.581	–	–
2018/02/05 07:00	0.307	5.50E−15	5.58E+10
2018/02/05 19:00	0.320	3.51E−16	9.12E+11
2018/02/06 07:00	0.513	5.78E−16	8.88E+11
2018/02/06 19:00	0.409	–	–
Mean source-term			6.40E+11

Calculation of source-term is based on the assumption of a single source of radioxenon. Source-terms are replaced by '–' where the simulation is not in good temporal agreement with the collection period

Figure 9

Yongbyon Research Reactor: JPX38 modelled activity concentration distribution, based on releases of 6.4E+11 Bq ^{133}Xe. The dashed red line represents an MDC of 0.28 mBq m^{-3}

simulations showed the station (JPX38) was sensitive to contributions from modelled emitters in North Korea. Simulations for the Japanese and Chinese NPPs and South Korean MIPF 'Kori' were cross-checked with detections at JPX38 and did not match well with the timing of the detections discussed here.

Using RASCA to assess a number of emissions from the Yongbyon reactor site and calculate a mean contribution for each collection period, it is possible to estimate a source-term for the Yongbyon site. The results of this analysis are given in Table 5. These results are based on a 2 h emission of constant rate, as used by the ATM pipeline, and calculated source-terms have been decay corrected to the emission start time. It was not possible to match every collection period to contributions from the ATM Pipeline simulations, but this does not mean that there is no contribution from Yongbyon during the collection periods where no dilution factor could be obtained, primarily due to the pipeline only simulating 4 × 2 h emissions. The uncertainties on these results are difficult to quantify, primarily due to the ATM (see Maurer et al. 2018; Eslinger et al. 2016). This result should therefore be treated cautiously as an 'upper limit' to the source-term, with at least ± 1 order of magnitude uncertainty. There are also a number of assumptions made as part of these calculations,
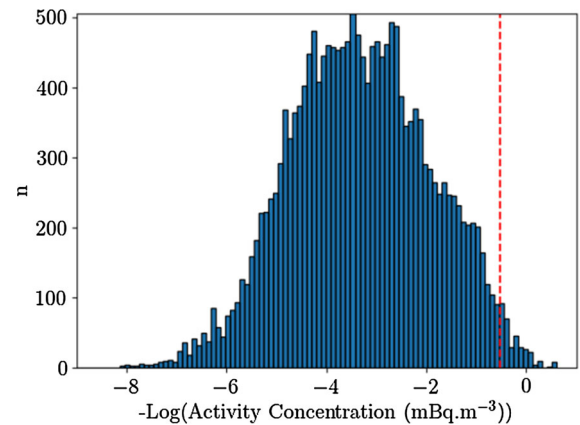
including the detections of each 'event' being wholly attributable to a single emission.

The calculated source-terms (see Table 5) are higher than expected, compared to that based on assumptions made in the literature. Given that it is unlikely for stack emission data from the Yongbyon reactor to be made available, definitive statements regarding the magnitude of the source are difficult to make, especially given the proximity of other local sources and their potential influence on JPX38.

Based on IMS data, the source-term has been estimated to be around 6.4E+11 Bq for ^{133}Xe, which shifts the contribution histogram such that a small fraction of the emissions from this site would be detected above the MDC. Figure 9 shows that a fraction of samples that would contain detectable levels of ^{133}Xe, based on emissions of 6.4E+11 Bq from the Yongbyon reactor facility. Applying a normal distribution shows that around 1.5 % of simulated collection periods have measurable levels of ^{133}Xe, increasing the MDCs for any ^{133}Xe, ^{131m}Xe and ^{133m}Xe that may be emitted from the DPRK nuclear test site. It is clear that assuming a release of 1E+10 Bq from Yongbyon results in no detections at JPX38 without interference from other releases. Emissions at broadly the same time from Yongbyon would be considerably more likely to affect the detectability of emissions from the test site.

A second series of detections were picked up in the RN Pipeline data meta-analysis, and a series of

Event ID	Est. start	Est. end	N	Detected
2019-01	22-01-2019	25-01-2019	5	^{133}Xe
2019-02	31-01-2019	01-02-2019	3	^{133}Xe
2019-03	12-03-2019	13-03-2019	3	^{133}Xe
2019-04	05-04-2019	07-04-2019	5	^{133}Xe, ^{135}Xe
2019-05	15-04-2019	17-04-2019	6	^{133}Xe
2019-06	01-05-2019	06-05-2019	7	^{133}Xe, ^{135}Xe
2019-07	26-05-2019	26-05-2019	7	^{133}Xe, ^{131m}Xe

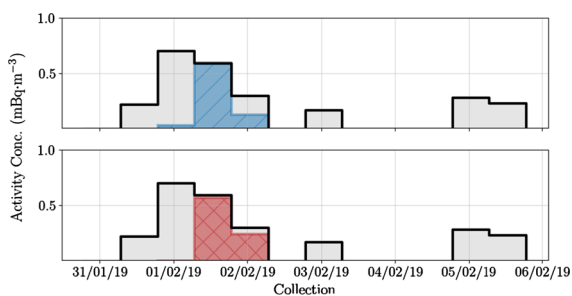N: Number of detections considered to be relevant to the 'event', above the MDC

Figure 10
Modelled detections based on ATM Pipeline simulations, for DPRK Test Site (^{133}Xe emission of 2E+11 Bq on 30-01-2019 0900 hrs, slashed blue shading) and Yongbyon (^{133}Xe emission of 9E+11 Bq on 30-01-2019 0900 hrs, hatched red shading). Real RN data measured data shown as a black line, where ^{133}Xe is detected above the critical limit

'events' have been identified, whereby there is more than one detection of one or more isotopes of radio-xenon. The events are summarised in Table 6. During the collection period of event ID 2019–02, JPX38 was sensitive to simulated emissions from the DPRK region as several simulated pipeline emissions contributed to the station significantly. Emissions from other locations, including Japan, South Korea and mainland China did not correlate well with the detections highlighted at JPX38.

Figure 10 shows the JPX38 radionuclide detections in January 2019, overlaid with simulated contributions from the test site and Yongbyon respectively. The simulations are not constrained to fit the detections, both are independent of one another and are taken directly from the ATM pipeline. The overlay shows that during this period, the station was sensitive to the DPRK region and emissions from either the test site or Yongbyon could explain the detections, however the pipeline emission profile is not representative of any possible real emission. The Yongbyon source-terms calculated from these detections are of comparable magnitude to the source-terms calculated using the 2018 detections, given in Table 5. As before, the source-term should be viewed as an 'upper limit' where the actual value could be lower and the detections are interfered by other background sources. The DPRK test site simulated source-term was calculated based on a 'best fit' approach; the value of 2E+11 Bq was determined as a maximum possible emission that could explain some of the detections, however since we can assume no test took place around this time, it is more likely associated with a contribution from Yongbyon and the simulations here suggest a source term of 9E+11 Bq. It may be possible to better constrain the source location through inverse modelling (De Meutter et al. 2018).

6. Discussion

Analysing radionuclide events on the IMS involves the interpretation of infrequent, sparse, low-level detections that are often unremarkable when compared to the measured *background* levels. The definition of an *event* is variable depending on the radionuclides frequently detected (and the magnitude thereof) at the location. Studies such as this should continue to be conducted to assess the sensitivity of IMS stations to sites of interest and known radio-xenon emitters.

Given the aforementioned limitations, event analysis should be treated on a case-by-case basis—there is no 'one size fits all' for radioxenon detections. To address the limitations in radioxenon detection at an IMS level, increased sensitivity is required; this could be achieved with a denser network of noble gas detectors, or a significant change in the detection limits of the noble gas sampling and detection systems used in the field, in order to obtain multi-isotope detections. Improved detection sensitivity (lower detection limits) of laboratory re-analysis would also greatly help, especially during

Expert Technical Analysis. Measurement of samples containing ^{133}Xe after an extended period of decay can (on most radioxenon detection systems) improve the detection sensitivity to meta-stable isomers such as ^{131m}Xe, as the interference from ^{133}Xe decreases with time. A detection of ^{131m}Xe can help in determining the origin of the radioxenon sample (Kalinowski et al. 2010).

The UK NDC RN & ATM Pipelines have been used to assess the sensitivity of the Takasaki RN IMS station to emissions of radioxenon from selected locations on the Korean peninsula. There are a number of potential emitters that influence (and could be used to explain) low level detections of ^{133}Xe at JPX38. It is clear that emissions from the Yongbyon nuclear reactor could be mis-identified as possible emissions from the test site where single isotopes are detected. The results presented are circumstantial due to a lack of information such as stack emission magnitude, isotopic composition and emission profile, however they demonstrate the relative sensitivity to a number of sites and how civil and (possible) non-civil emissions can be detected and interpreted on the IMS.

If selected detections at JPX38 were solely resulting from the Yongbyon nuclear facility, then a source-term of at least 1E+11 Bq would be required. We demonstrated 6.4E+11 Bq and 9E+11 Bq simulated emissions contributing to JPX38 in January/February 2018 and 2019 respectively.

As part of an NDC's role to interpret IMS data that may be indicative of a violation to the Treaty, due consideration must be given to known (modelled) and unknown (not currently modelled) sources of radioxenon. This work will be expanded to include considerations of all known emitters of radioxenon and their impact on all IMS radioxenon stations, in order to better understand the effect of civil radioxenon emitters on the ability of the IMS to detect an underground nuclear test.

Acknowledgements

Publisher's Note Springer Nature remains neutral with regard to jurisdictional claims in published maps and institutional affiliations.

References

Achim, P., Generoso, S., Morin, M., Gross, P., Le Petit, G., & Moulin, C. (2016). Characterization of Xe-133 global atmospheric background: Implications for the international monitoring system of the comprehensive nuclear-test-ban treaty. *Journal of Geophysical Research: Atmospheres*, *121*, 4951–4966.

Auer, M., Axelsson, A., Blanchard, X., Bowyer, T. W., Brachet, G., Bulowski, Y., et al. (2004). Intercomparison experiments of systems for the measurement of xenon radionuclides in the atmosphere. *Applied Radiation and Isotopes*, *60*, 863–877.

Axelsson, A. & Ringbom, A. (2003). Xenon Air Activity Concentration Analysis from Coincidence Data, FOI Report, FOI-R-0913-SE.

Axelsson, A., & Ringbom, A. (2014). On the calculation of activity concentrations and nuclide ratios from measurements of atmospheric radioactivity. *Applied Radiation and Isotopes*, *92*, 12–17.

Bowyer, T. W., Kephart, R., Eslinger, P. W., Friese, J. I., Miley, H. S., & Saey, P. R. J. (2013). Maximum reasonable radioxenon releases from medical isotope production facilities and their effect on monitoring nuclear explosions. *Journal of Environmental Radioactivity*, *115*, 192–200.

Bowyer, T. W., Schlosser, C., Abel, K. H., Auer, M., Hayes, J. C., Heimbigner, T. R., et al. (2002). Detection and analysis of xenon isotopes for the comprehensive nuclear-test-ban treaty international monitoring system. *Journal of Environmental Radioactivity*, *59*, 139–151.

Cagniant, A., Topin, S., Le Petit, G., Gross, P., Delaune, O., Phillippe, T., et al. (2018). SPALAX NG: A breakthrough in radioxenon field measurement. *Applied Radiation and Isotopes*, *134*, 461–465.

Certification and surveillance assessment of radionuclide laboratories for particulate and noble gas analysis, CTBTO Report, CTBT/PTS/INF.96/Rev.9, (2012).

Comley, C., & Price, O. (2003). CTBT radionuclide verification and the British laboratory, Vertic Verification Yearbook. http://www.vertic.org/media/Archived_Publications/Yearbooks/2003/VY03_Comley-Price.pdf. Accessed Dec 2019.

Currie, L. A. (1968). Limits for qualitative detection and quantitative determination-application to radiochemistry. *Analytical Chemistry*, *40*(3), 586–593.

De Geer, L. E. (1999). CTBT relevant radionuclides. CTBTO Preparatory Commission Techincal Report 1999-02.

De Meutter, P., Camps, J., & Delcloo, A. (2018). Source localisation and its uncertainty quantification after the third DPRK nuclear test. *Scientific Reports*, *8*, 10155.

Deshmukh, N., Prinke, A., Miller, B., & McIntyre, J. (2017). Comparison of new and existing algorithms for the analysis of 2D radioxenon beta gamma spectra. *Journal of Radioanalytical and Nuclear Chemistry*, *311*, 1849–1857.

England, T. R. & Rider, B. F. (1993). Evaluation and Compilation of Fission Product Yields, LA-UR-94-3106; ENDF-349

Eslinger, P. W., et al. (2016). International challenge to predict the impact of radioxenon releases from medical isotope production on a comprehensive Nuclear Test Ban Treaty sampling station. *Journal of Environmental Radioactivity*, *157*, 41–51.

Fontaine, J. P., Pointurier, F., Blanchard, X., & Taffary, T. (2004). Atmospheric xenon radioactive isotope monitoring. *Journal of Environmental Radioactivity*, *72*, 129–135.

Hoffman, I., & Berg, R. (2018). Medical isotope production, research reactors and their contribution to the global xenon background. *Journal of Radioanalytical and Nuclear Chemistry*, *318*, 165–173.

Kalinowski, M., Axelsson, A., Bean, M., Blanchard, X., & Bowyer, T. W. (2010). Discrimination of nuclear explosions against civilian sources based on atmospheric xenon isotopic activity ratios. *Pure and Applied Geophysics*, *167*, 517–539.

Kalinowski, M. B., & Tuma, M. P. (2009). Global radioxenon emission inventory based on nuclear power reactor reports. *Journal of Environmental Radioactivity*, *100*, 58–70.

Matthews, M., & Schulze, J. (2001). The radionuclide monitoring system of the comprehensive nuclear-test-ban treaty organisation: From sample to product. *Kerntechnik*, *66*(3), 102–112.

Maurer, C., et al. (2018). International challenge to model the long-range transport of radioxenon released from medical isotope production to six comprehensive Nuclear Test-Ban Treaty monitoring stations. *Journal of Environmental Radioactivity*, *192*, 667–686.

Miskel, J. A. (1964). Characteristics of radioactivity produced by nuclear explosives. In *Engineering with nuclear explosives, Proceedings of the third plowshare symposium* (pp. 153–160).

Nuclear Power Reactors in the World, International Atomic Energy Agency (IAEA), 2019 Edn, IAEA-RDS-2/39, (2019).

Ringbom, A., Axelsson, A., Aldener, M., Auer, M., Bowyer, T. W., Fritioff, T., et al. (2014). Radioxenon detections in the CTBT international monitoring system likely related to the announced nuclear test in North Korea on February 12, 2013. *Journal of Environmental Radioactivity*, *128*, 47–63.

Ringbom, A., Larson, T., Axelsson, A., Elmgren, K., & Johansson, C. (2003). SAUNA: A system for automatic sampling, processing, and analysis of radioactive xenon. *Nuclear Instrumentation and Methods in Physics Research Section A*, *508*, 542–553.

Saey, P. R. J. (2009). The influence of radiopharmaceutical isotope production on the global radioxenon background. *Journal of Environmental Radioactivity*, *100*, 396–406.

Status of Provisional Technical Secretariat Work on International Monitoring System Stations and Radionuclide Laboratories, CTBTO Report, CTBT/PTS/INF.142/Rev.45, (2020)

Stein, A. F., Draxler, R. R., Rolph, G. D., Stunder, B. J. B., Cohen, M. D., & Ngan, F. (2015). NOAA's HYSPLIT atmospheric transport and dispersion modeling system. *Bulletin of the American Meteorological Society*, *96*, 2059–2077.

UNGA (1996) United Nations General Assembly Resolution Number 50/245. UN, New York, USA.

Werth, D., & Buckley, R. (2017). Characterising the detectability of emission signals from a North Korean nuclear detonation. *Journal of Environmental Radioactivity*, *169–170*, 214–220.